Supplementary material

Synthesis strategies for BaCe0.7Zr0.1Y0.1Yb0.1O3-δ for the development of high-conducting Solid Oxide Cell electrolyte

F. Bagioni[1,2], E. Mercadelli[1], A. Bartoletti[1], P. Pinasco[1], M. Ardit[3], N. Precisvalle[4], S. Massardo[5], S. Presto[5], M. Viviani[5*], A. Gondolini[1*], A. Sanson[1]

[1] National Research Council of Italy, Institute of Science, Technology and Sustainability for Ceramics (ISSMC) of the National Research Council (CNR), Via Granarolo 64, 48018 Faenza (RA), Italy

[2] Department of Chemistry, Life Sciences and Environmental Sustainability, University of Parma, via Università, 12 - I 43121 Parma, Italy

[3] Department of Geosciences, University of Padova, Via Gradenigo 6, IT-35131 Padova, Italy

[4] Department of Physics and Earth Sciences, University of Ferrara, v. Saragat 1, I-44122, Ferrara, Italy

[5] National Research Council of Italy, Institute of Condensed Matter Chemistry and Energy Technologies (ICMATE) of the National Research Council (CNR), c/o DICCA-UNIGE, Via all'Opera Pia 15, 16145 Genova, Italy

*Corresponding authors: email address: angela.gondolini@cnr.it, massimo.viviani@cnr.it

Details on the Rietveld refinements

The quantification of the identified phases within each sample was conducted through a full-profile fitting analyses using the fundamental-parameter (FP) Rietveld approach (TOPAS Bruker AXS, v7.0, Cheary and Coelho 1992; Cheary et al. 2004; Rietveld 1967, 1969). The starting atomic models were derived from Pagnier et al. (2000) for the cubic and orthorhombic perovskite phases (s.g. *Pm*-3*m* and *Imma*, respectively), from Knight and Bonanos (1995) for the orthorhombic perovskite phase (s.g. *Pmcn*), and from Takeuchi et al. (2000) for the monoclinic perovskite phase (s.g. *I*2/*m*). The atomic models for other associated phases, which occurred in some samples as unreacted precursors, were derived from Coduri et al. (2013) for the cubic Y_2O_3 phase (s.g. *Ia*-3), from Saiki et al. (1985) for the cubic Yb_2O_3 phase (s.g. *Ia*-3), from Szymanik et al. (1998) for the trigonal $Ba_3Y_4O_9$ phase (s.g. *R*3H), and from Antao and Hassan (2009) for the orthorhombic $BaCO_3$ phase (s.g. *Pcmn*).

Known instrumental parameters (*e.g.*, goniometer radius, slit sizes, geometrical parameters of the X-ray tube, etc.) were employed to calculate the instrumental contribution to the peak profiles. Additionally, specimen-related Lorentzian broadening was extracted from the observed peak profiles to assess the crystallite size of the main phases through the integral breadth approach (Laue, 1926). An instrumental zero error was fixed at the value determined using the Si 640e NIST standard, and refinement included a sample displacement correction and a 5-term Chebyshev polynomial to model the background. In addition to the aforementioned variables, the multiphase refinements included scale factors and unit-cell parameters for each identified phase.

The Rietveld refinement plots of the *LEM*, *HEM* and *MSG* powder samples data collected at *RT* are shown in Figure S1, while those for the *LEM*, *HEM* and *MSG* pellet samples are shown in Figure S2.

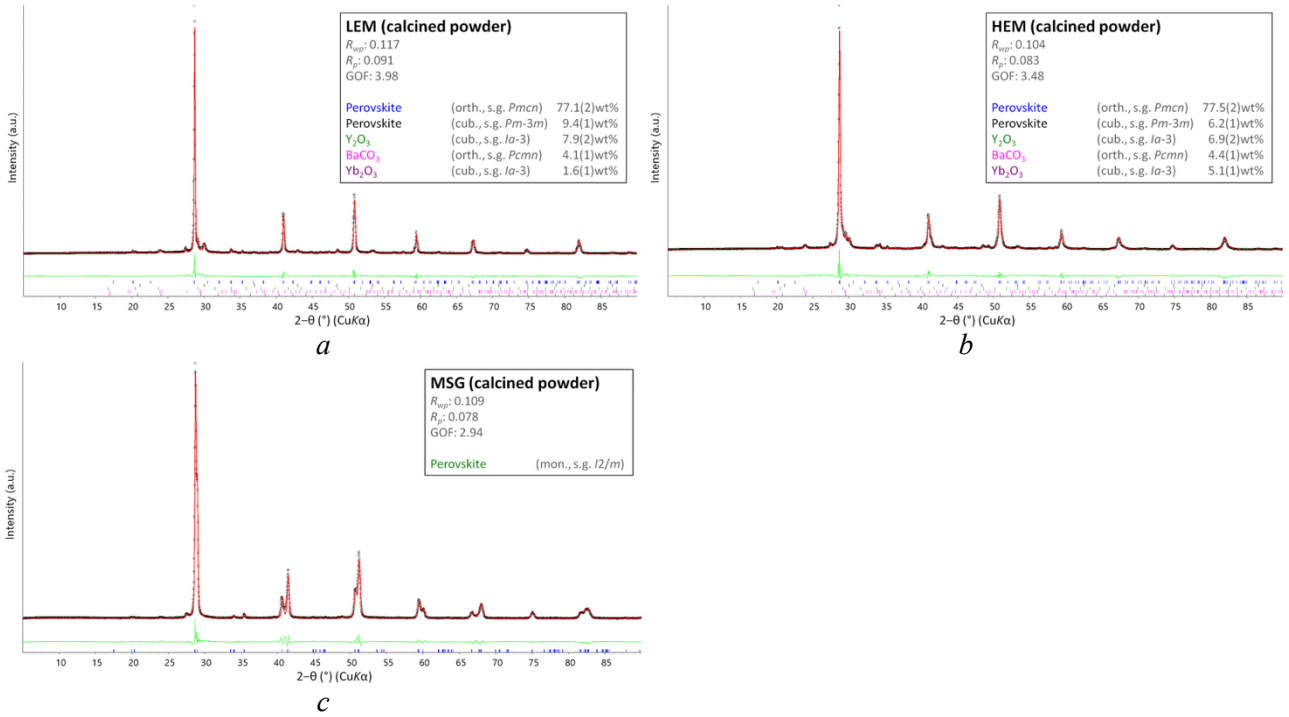

Figure S1. Rietveld refinement plot for the *LEM*, *HEM* and *MSG* powder samples collected at *RT*. The experimental data are indicated by circles (black), the calculated pattern is the solid line (red), and the lower curve (green) is the weighted difference between the observed and calculated patterns. Vertical ticks mark the position of the reflection for the identified phases.

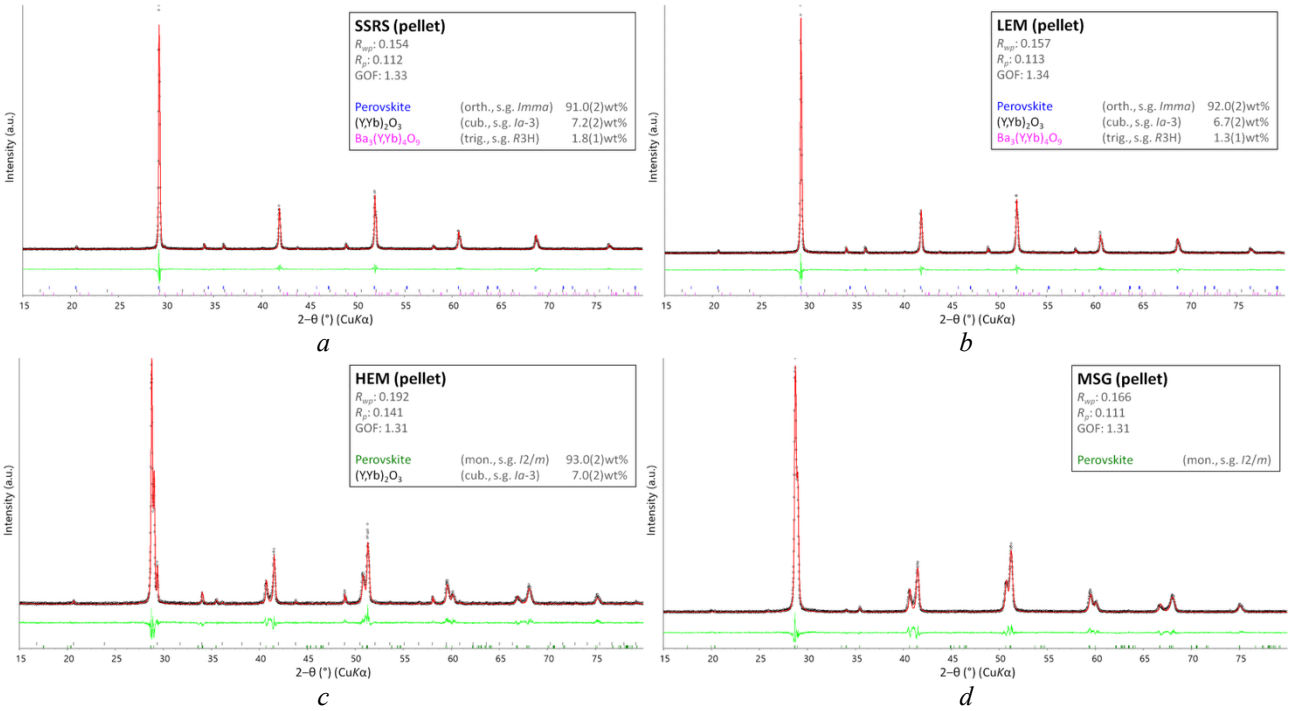

Figure S2. Rietveld refinement plot for the *LEM*, *HEM* and *MSG* pellet samples collected at *RT*. The experimental data are indicated by circles (black), the calculated pattern is the solid line (red), and the lower curve (green) is the weighted difference between the observed and calculated patterns. Vertical ticks mark the position of the reflection for the identified phases.

References

Antao, S. M., & Hassan, I. (2009). The orthorhombic structure of $CaCO_3$, $SrCO_3$, $PbCO_3$ and $BaCO_3$: Linear structural trends. The Canadian Mineralogist, 47(5), 1245-1255. https://doi.org/10.3749/canmin.47.5.1245

Cheary, R. W., & Coelho, A. (1992). A fundamental parameters approach to X-ray line-profile fitting. Journal of Applied Crystallography, 25(2), 109-121. https://doi.org/10.1107/S0021889891010804

Cheary, R. W., Coelho, A. A., & Cline, J. P. (2004). Fundamental parameters line profile fitting in laboratory diffractometers. Journal of Research of the National Institute of Standards and Technology, 109(1), 1. https://doi.org/10.6028/jres.109.002

Coduri, M., Scavini, M., Allieta, M., Brunelli, M., & Ferrero, C. (2013). Defect structure of Y-doped ceria on different length scales. Chemistry of Materials, 25(21), 4278-4289. https://doi.org/10.1021/cm402359d

Knight, K. S., & Bonanos, N. (1995). The crystal structures of some doped and undoped alkaline earth cerate perovskites. Materials Research Bulletin, 30(3), 347-356. https://doi.org/10.1016/0025-5408(95)00009-7

Laue, M. V. (1926). VI. Lorentz-Faktor und Intensitätsverteilung in Debye-Scherrer-Ringen. Zeitschrift für Kristallographie-Crystalline Materials, 64(1-6), 115-142. https://doi.org/10.1524/zkri.1926.64.1.115

Pagnier, T., Charrier-Cougoulic, I., Ritter, C., & Lucazeau, G. (2000). A neutron diffraction study of $BaCe_xZr_{1-x}O_3$. The European Physical Journal-Applied Physics, 9(1), 1-9. https://doi.org/10.1051/epjap:2000192

Rietveld, H. M. (1967). Line profiles of neutron powder-diffraction peaks for structure refinement. Acta Crystallographica, 22(1), 151-152. https://doi.org/10.1107/S0365110X67000234

Rietveld, H. M. (1969). A profile refinement method for nuclear and magnetic structures. Journal of applied Crystallography, 2(2), 65-71. https://doi.org/10.1107/S0021889869006558

Saiki, A., Ishizawa, N., Mizutani, N., & Kato, M. (1985). Structural change of C-rare earth sesquioxides Yb_2O_3 and Er_2O_3 as a function of temperature. Journal of the Ceramic Society of Japan, 93(10), 649-654. https://doi.org/10.2109/jcersj1950.93.1082_649

Szymanik, B., Buckley, R. G., Trodahl, H. J., & Davis, R. L. (1998). Structure and decomposition of ceramic $Ba_3Y_4O_9$. Solid state ionics, 109(3-4), 223-228. https://doi.org/10.1016/S0167-2738(98)00087-3

Takeuchi, K., Loong, C. K., Richardson Jr, J. W., Guan, J., Dorris, S. E., & Balachandran, U. (2000). The crystal structures and phase transitions in Y-doped $BaCeO_3$: Their dependence on Y concentration and hydrogen doping. Solid State Ionics, 138(1-2), 63-77. https://doi.org/10.1016/S0167-2738(00)00771-2